THE ASTROPHYSICAL JOURNAL, 530:L111–L114, 2000 February 20
© 2000. The American Astronomical Society. All rights reserved. Printed in U.S.A.

FIRST LIGHT MEASUREMENTS OF CAPELLA WITH THE LOW-ENERGY TRANSMISSION GRATING SPECTROMETER ABOARD THE *CHANDRA X-RAY OBSERVATORY*

A. C. BRINKMAN, C. J. T. GUNSING, J. S. KAASTRA, R. L. J. VAN DER MEER, R. MEWE, F. PAERELS,[1]
A. J. J. RAASSEN,[2] AND J. J. VAN ROOIJEN
Space Research Organization of the Netherlands (SRON), Sorbonnelaan 2,
3584 CA Utrecht, Netherlands
H. BRÄUNINGER, W. BURKERT, V. BURWITZ, G. HARTNER, AND P. PREDEHL
Max-Planck-Institut für Extraterrestrische Physik, Postfach 1603,
D-85740 Garching, Germany
J.-U. NESS AND J. H. M. M. SCHMITT
Universität Hamburg, Gojenbergsweg 122, D-21029 Hamburg, Germany
AND
J. J. DRAKE, O. JOHNSON, M. JUDA, V. KASHYAP, S. S. MURRAY, D. PEASE, P. RATZLAFF, AND B. J. WARGELIN
Harvard-Smithsonian Center for Astrophysics, 60 Garden Street, Cambridge, MA 02138
Received 1999 November 23; accepted 1999 December 23; published 2000 January 25

ABSTRACT

We present the first X-ray spectrum obtained by the Low-Energy Transmission Grating Spectrometer (LETGS) aboard the *Chandra X-Ray Observatory*. The spectrum is of Capella and covers a wavelength range of 5–175 Å (2.5–0.07 keV). The measured wavelength resolution, which is in good agreement with ground calibration, is $\Delta\lambda \simeq 0.06$ Å (FWHM). Although in-flight calibration of the LETGS is in progress, the high spectral resolution and unique wavelength coverage of the LETGS are well demonstrated by the results from Capella, a coronal source rich in spectral emission lines. While the primary purpose of this Letter is to demonstrate the spectroscopic potential of the LETGS, we also briefly present some preliminary astrophysical results. We discuss plasma parameters derived from line ratios in narrow spectral bands, such as the electron density diagnostics of the He-like triplets of carbon, nitrogen, and oxygen, as well as resonance scattering of the strong Fe XVII line at 15.014 Å.

Subject headings: instrumentation: spectrographs — line: identification — plasmas — stars: coronae — stars: individual (Capella) — X-rays: stars

1. INTRODUCTION

The Low-Energy Transmission Grating Spectrometer (LETGS) consists of three components of the *Chandra Observatory*: the High-Resolution Mirror Assembly (Van Speybroeck et al. 1997), the Low-Energy Transmission Grating (LETG; Brinkman et al. 1987, 1997; Predehl et al. 1997), and the spectroscopic array of the High-Resolution Camera (HRC-S; Murray et al. 1997). The LETG, designed and manufactured in a collaborative effort of the Space Research Organization of the Netherlands and the Max-Plank-Institut für Extraterrestrische Physik in Germany, consists of a toroidally shaped structure that supports 180 grating modules. Each module holds three 1.5 cm diameter grating facets, which have a line density of 1008 lines mm^{-1}. The three flat detector elements of the HRC-S, each 10 cm long and 2 cm wide, are tilted to approximate the Rowland focal surface at all wavelengths, ensuring a nearly coma-free spectral image. The detector can be moved in the cross-dispersion direction and along the optical axis to optimize the focus for spectroscopy.[3]

An image of the LETG spectrum is focused on the HRC-S with zeroth order at the focus position and dispersed positive and negative orders symmetric on either side of it. The dispersion is 1.15 Å mm^{-1} in first spectral order. The spectral width in the cross-dispersion direction is minimal at zeroth order and increases at larger wavelengths due to the intrinsic astigmatism of the Rowland circle spectrograph. The extraction of the spectrum from the image is done by applying a spatial filter around the spectral image and constructing a histogram of counts versus position along the dispersion direction. The background is estimated from areas on the detector away from the spectral image and can be reduced by filtering events by pulse height.

2. FIRST LIGHT SPECTRUM

Capella is a binary system at a distance of 12.9 pc consisting of G8 and G1 giants with an orbital period of 104 days (Hummel et al. 1994). It is the brightest quiescent coronal X-ray source in the sky after the Sun and is therefore an obvious line source candidate for first light and for instrument calibration. X-rays from Capella were discovered in 1975 (Catura, Acton, & Johnson 1975; Mewe et al. 1975), and subsequent satellite observations provided evidence for a multitemperature component plasma (see, e.g., Mewe 1991 for references). Recent spectra were obtained with the *Extreme-Ultraviolet Explorer* (*EUVE*) longward of 70 Å with a resolution of about 0.5 Å (Dupree et al. 1993; Schrijver et al. 1995).

The LETG first light observation of Capella was performed on 1999 September 6 (00^h27^m–10^h04^m UT) with LETG and HRC-S. For the analysis we use a composite of six observations obtained in the week after first light, with a total observing time of 95 ks. The HRC-S output was processed through standard pipeline processing. For LETG/HRC-S events, only the

[1] Present address: Columbia University, New York, NY.
[2] Also at Astronomical Institute "Anton Pannekoek," Kruislaan 403, 1098 SJ Amsterdam, Netherlands.
[3] Further information on LETGS components is found in the *AXAF* Observatory Guide (http://asc.harvard.edu/udocs/) and at the *Chandra* X-Ray Center calibration Web site (http://asc.harvard.edu/cal/).

product of the wavelength and diffraction order is known because no diffraction order information can be extracted. Preliminary analysis of the pipeline output immediately revealed a beautiful line-rich spectrum. The complete background-subtracted, negative-order spectrum between 5 and 175 Å is shown in Figure 1. Line identifications were made using previously measured and/or theoretical wavelengths from the literature. The most prominent lines are listed in Table 1.

The spectral resolution $\Delta\lambda$ of the LETGS is nearly constant when expressed in wavelength units, and therefore the resolving power $\lambda/\Delta\lambda$ is greatest at long wavelengths. With the current uncertainty of the LETGS wavelength scale of about 0.015 Å, this means that the prominent lines at 150 and 171 Å could be used to measure Doppler shifts as small as 30 km s^{-1}, such as may occur during stellar flare mass ejections, once the absolute wavelength calibration of the instrument has been established. This requires, however, that line rest-frame wavelengths are accurately known and that effects such as the orbital velocity of the Earth around the Sun are taken into account. Higher order lines, such as the strong O VIII Lyα line at 18.97 Å, which is seen out to sixth order, can also be used.

3. DIAGNOSTICS

A quantitative analysis of the entire spectrum by multitemperature fitting or differential emission measure modeling yields a detailed thermal structure of the corona, but this requires accurate detector efficiency calibration which has not yet been completed. However, some diagnostics based on intensity ratios of lines lying closely together can already be applied. In this Letter we consider the helium-like line diagnostic and briefly discuss the resonance scattering in the Fe XVII λ15.014 line.

3.1. *Electron Density and Temperature Diagnostics*

Electron densities n_e can be measured using density-sensitive spectral lines originating from metastable levels, such as the forbidden (f) $2^3S \rightarrow 1^1S$ line in helium-like ions. This line and the associated resonance (r) $2^1P \rightarrow 1^1S$ and intercombination (i) $2^3P \rightarrow 1^1S$ line make up the so-called helium-like "triplet" lines (Gabriel & Jordan 1969; Pradhan 1982; Mewe, Gronenschild, & van den Oord 1985). The intensity ratio $(i + f)/r$ varies with electron temperature T, but more importantly, the ratio i/f varies with n_e due to the collisional coupling between the 2^3S and 2^3P level.

The LETGS wavelength band contains the He-like triplets from C, N, O, Ne, Mg, and Si (~40, 29, 22, 13.5, 9.2, and 6.6 Å, respectively). However, the Si and Mg triplets are not sufficiently resolved and the Ne IX triplet is too heavily blended with iron and nickel lines for unambiguous density analysis. The O VII lines are clean (see Fig. 2), and the C V and N VI lines can be separated from the blends by simultaneous fitting of all lines. These triplets are suited to diagnose plasmas in the range $n_e = 10^8$–10^{11} cm^{-3} and $T \sim 1$–3 MK. For the C, N, and O triplets the measured i/f ratios are 0.38 ± 0.14, 0.52 ± 0.15, and 0.250 ± 0.035, respectively, which imply (Pradhan 1982) n_e (in 10^9 cm^{-3}) $= 2.8 \pm 1.3$, 6 ± 3, and $\lesssim 5$ ($1\ \sigma$ upper limit), respectively, for typical temperatures as indicated by the $(i + f)/r$ ratios of 1, 1, and 3 MK, respectively. This concerns the lower temperature part of a multitemperature structure which also contains a hot (~6–8 MK) and dense ($\gtrsim 10^{12}$ cm^{-3}) compact plasma component (see § 3.2). The derived densities are comparable to those of active regions on the Sun with a temperature of a few MK. Figure 2 shows a fit to the O VII triplet measured in the −1 order. The He-like triplet diagnostic, which was first applied to the Sun (e.g., Acton et al. 1972; Wolfson, Doyle, & Phillips 1983), has now for the first time been applied to a star other than the Sun.

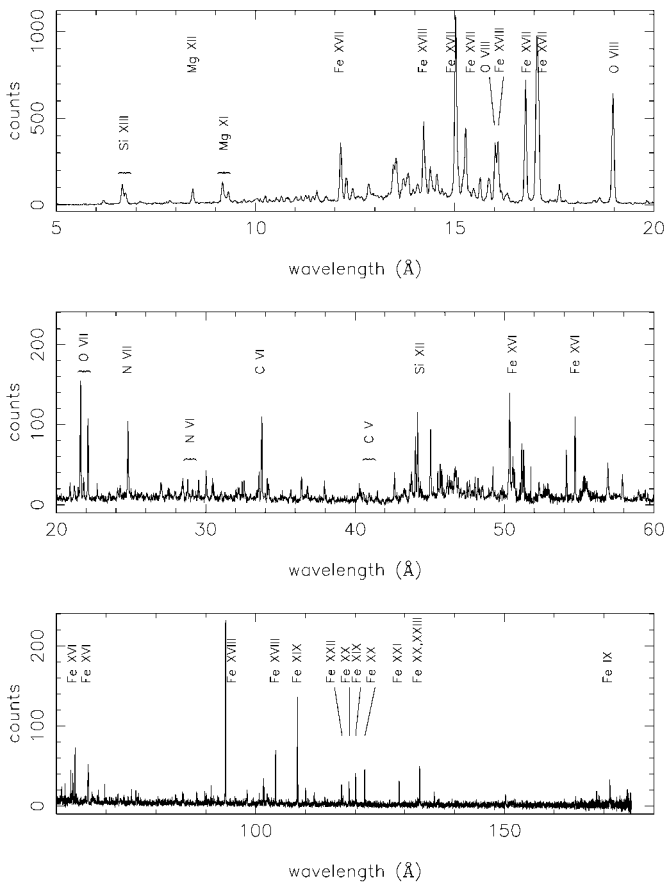

FIG. 1.—Complete LETGS spectrum of Capella, split into three parts for clarity. Note the difference in x and y scale for the three parts. Indicated in the plot are the triplets discussed in the text and a selection of the Fe lines at longer wavelengths. The hundred strongest lines are listed in Table 1.

The long-wavelength region of the LETGS between 90 and 150 Å contains a number of density-sensitive lines from $2l$–$2l'$ transitions in the Fe-L ions Fe XX–Fe XXII, which provide density diagnostics for relatively hot ($\gtrsim 5$ MK) and dense ($\gtrsim 10^{12}$ cm^{-3}) plasmas (Mewe et al. 1985; Mewe, Lemen, & Schrijver 1991; Brickhouse, Raymond, & Smith 1995). These have been applied in a few cases to *EUVE* spectra of late-type stars and in the case of Capella have suggested densities more than 2 orders of magnitude higher than found here for cooler plasma (Dupree et al. 1993; Schrijver et al. 1995). These diagnostics will also be applied to the LETGS spectrum as soon as the long-wavelength efficiency calibration is established.

3.2. *The* 15–17 Å *Region: Resonance Scattering of* Fe XVII*?*

Transitions in Ne-like Fe XVII yield the strongest emission lines in the range 15–17 Å (see Fig. 1). In principle, the optical depth τ in the 15.014 Å line can be obtained by applying a simplified escape-factor model to the ratio of the Fe XVII λ15.014 resonance line with a large oscillator strength to a presumably optically thin Fe XVII line with a small oscillator strength. We use the 15.265 Å line because the 16.780 Å line can be affected by radiative cascades (D. A. Liedahl 1999, private communication). Solar physicists have used this tech-

TABLE 1

COMPARISON OF MEASURED AND THEORETICAL VALUES OF THE STRONGEST LINES IN THE CAPELLA SPECTRUM AS SHOWN IN FIGURE 1

λ_{obs}[a] (Å)	λ_{pred}[a] (Å)	log (T_m)[b]	I[c] (10^{-3} counts s^{-1})	Ion	Line Identification[d]	λ_{obs}[a] (Å)	λ_{pred}[a] (Å)	log (T_m)[b]	I[c] (10^{-3} counts s^{-1})	Ion	Line Identification[d]
6.65	6.65	7.00	5.1	Si XIII	He4w	24.79	24.78	6.30	4.4	N VII	H1AB
6.74	6.74	7.00	2.9	Si XIII	He6z	28.78	28.79	6.20	1.1	N VI	He4w
8.42	8.42	7.00	4.6	Mg XII	H1AB	29.52	29.53	6.20	0.9	N VI	He6z
9.16	9.17	6.80	6.2	Mg XI	He4w	30.02	30.03	6.70	1.8	Fe XVII	3C(2)
9.31	9.32	6.80	3.1	Mg XI	He6z	33.74	33.74	6.10	4.9	C VI	H1AB
11.54b	11.55	6.60	3.5	Ne IX	He3A	34.10	34.10	6.70	1.5	Fe XVII	3G(2)
	11.53	6.85	...	Fe XVIII	F22	34.20	34.20	6.70	1.1	Fe XVII	M2(2)
12.14b	12.13	6.80	16.8	Ne X	H1AB	36.40b	36.37	6.70	1.4	Fe XVII	4C(3)
	12.12	6.75	...	Fe XVII	4C		36.40	6.30	...	S XII	B6A
12.27b	12.26	6.75	6.6	Fe XVII	4D	37.94	37.95	6.50	1.1	O VIII	H1AB(2)
	12.29	7.00	...	Fe XXI	C13	44.03b	44.02	6.30	3.3	Si XII	Li6A
12.43	12.43	6.70	3.5	Ni XIX	Ne5		44.05	6.10	...	Mg X	Li2
12.48b	12.83	7.00	4.9	Fe XX	N16	44.16	44.17	6.30	4.9	Si XII	Li6B
	12.85	7.00	...	Fe XX	N15	45.03	45.04	6.70	4.2	Fe XVII	3C(3)
13.46	13.45	6.60	9.7	Ne IX	He4w	45.68	45.68	6.30	1.9	Si XII	Li7A
13.53b	13.52	6.90	11.5	Fe XIX	O1-68	50.31	50.35	6.50	5.3	Fe XVI	Na6A
	13.51	6.90	...	Fe XIX	O1-71	50.55b	50.53	6.20	2.2	Si X	B6A
	13.55	6.90	...	Ne IX	He5xy		50.56	6.50	...	Fe XVI	Na6B
13.71	13.70	6.60	6.6	Ne IX	He6z	51.15	51.17	6.70	2.7	Fe XVII	3G(3)
13.82b	13.83	6.70	7.5	Fe XVII	3A	51.27	51.30	6.70	2.9	Fe XVII	M2(3)
	13.84	6.90	...	Fe XIX	O1-50	54.12	54.14	6.50	2.9	Fe XVI	Na7B
14.07	14.06	6.70	4.2	Ni XIX	Ne8AB	54.71	54.73	6.50	4.4	Fe XVI	Na7A
14.22	14.21	6.80	18.0	Fe XVIII	F1-56, 55	56.89	56.92	6.50	1.8	O VIII	H1AB(3)
14.27	14.26	6.80	5.3	Fe XVIII	F1-52, 53	60.04	60.06	6.70	1.3	Fe XVII	3C(4)
14.38b	14.38	6.80	6.2	Fe XVIII	F12	62.84	62.88	6.50	2.0	Fe XVI	Na8B
	14.36	6.80	...	Fe XVIII	F2-57, 58	63.68	63.72	6.50	2.9	Fe XVI	Na8A
14.56b	14.54	6.80	5.3	Fe XVIII	F10	66.37	66.37	6.50	2.7	Fe XVI	Na9A
	14.56	6.80	...	Fe XVIII	F9	68.20	68.22	6.70	1.0	Fe XVII	3G(4)
15.02	15.01	6.70	44.2	Fe XVII	3C	68.40	68.40	6.70	1.2	Fe XVII	M2(4)
15.18b	15.18	6.60	3.4	O VIII	H3	75.06	75.07	6.70	0.8	Fe XVII	3C(5)
	15.21	6.90	...	Fe XIX	O4	75.87	75.89	6.50	0.9	O VIII	H1AB(4)
15.27	15.27	6.70	16.7	Fe XVII	3D	85.24	85.28	6.70	0.8	Fe XVII	3G(5)
15.46	15.46	6.70	3.1	Fe XVII	3E	85.44	85.50	6.70	0.6	Fe XVII	M2(5)
15.64	15.63	6.80	6.2	Fe XVIII	F7	90.08	90.08	6.70	1.0	Fe XVII	3C(6)
15.83	15.83	6.80	4.3	Fe XVIII	F6	93.91	93.92	6.80	12.4	Fe XVIII	F4A
15.88	15.87	6.80	4.4	Fe XVIII	F5	94.84	94.87	6.50	0.4	O VIII	H1AB(5)
16.02b	16.01	6.60	14.6	O VIII	H2	101.55	101.55	6.90	2.5	Fe XIX	O6B
	16.00	6.80	...	Fe XVIII	F4	102.30	102.33	6.70	0.8	Fe XVII	3G(6)
16.08b	16.08	6.80	16.0	Fe XVIII	F3	102.57	102.60	6.70	0.4	Fe XVII	M2(6)
	16.11	6.90	...	Fe XIX	O2	103.94	103.94	6.70	4.4	Fe XVIII	F4B
16.30b	16.34	6.70	2.2	Fe XVII	E2L	108.35	108.37	6.90	6.1	Fe XIX	O6A
	16.31	6.80	...	Fe XVIII	F3-62	113.79	113.84	6.50	0.5	O VIII	H1AB(6)
16.78	16.78	6.70	27.9	Fe XVII	3F	117.14	117.17	7.10	1.2	Fe XXII	B11
17.05	17.06	6.70	30.5	Fe XVII	3G	118.69	118.66	7.00	1.4	Fe XX	N6C
17.10	17.10	6.70	29.5	Fe XVII	M2	119.99	120.00	6.90	1.8	Fe XIX	O6D
17.62	17.63	6.80	4.4	Fe XVIII	F1	121.86	121.83	7.00	2.0	Fe XX	N6B
18.62b	18.63	6.80	2.0	Mg XI	He6z(2)	128.74	128.74	7.00	1.6	Fe XXI	C6A
	18.63	6.30	...	O VII	He3A	132.86b	132.85	7.00	4.0	Fe XX	N6A
18.96	18.97	6.50	28.7	O VIII	H1AB		132.85	7.10	...	Fe XXIII	Be13A
21.61	21.60	6.30	6.5	O VII	He4w(r)	150.09	150.10	5.50	0.5	O VI	Li5AB
21.82	21.80	6.30	1.1	O VII	He5xy(i)	171.06	171.08	5.80	2.2	Fe IX	A4
22.11	22.10	6.30	4.5	O VII	He6z(f)						

NOTE.—For wavelengths and line identifications, see Phillips et al. 1999 (solar and laboratory measurements between 5 and 20 Å), Mason et al. 1984 (solar observations between 90 and 175 Å), and Mewe et al. 1985 and Mewe, Kaastra, & Liedahl 1995 (complete wavelength range in the MEKAL spectral code).

[a] λ_{obs}, λ_{pred}: observed and predicted line wavelengths; b = blend with indication of the most prominent lines in order of estimated decreasing strength.

[b] T_m = temperature (in kelvins) of maximum line formation.

[c] I = raw line intensity. Note that these are included to illustrate approximate observed relative line strengths and do not represent definitive measurements.

[d] Number in parentheses (m) indicates diffraction order $m > 1$.

nique to derive the density in active regions on the Sun (e.g., Saba et al. 1999; Phillips et al. 1996, 1997).

Various theoretical models predict 15.014/15.265 ratio values in the range 3.3–4.7 with only a slow variation ($\lesssim$5%) with temperature or energy in the region 2–5 MK or 0.1–0.3 keV (Brown et al. 1998; Bhatia & Doschek 1992). The fact that most ratios observed in the Sun typically range from 1.5 to 2.8 (Brown et al. 1998 and references above), significantly lower than the theoretical ratios, supports claims that in solar active regions the 15.014 Å line is affected by resonant scattering. The 15.014/15.265 ratio, which was recently measured in the Livermore electron beam ion trap (EBIT; Brown et al. 1998) and ranges from 2.77 to 3.15 (with individual uncertainties of about ± 0.2) at energies between 0.85 and 1.3 keV, is significantly lower than calculated values. Although the EBIT results do not include probably minor contributions from processes such as dielectronic recombination satellites and resonant excitation, this may imply that the amount of solar scattering has been overestimated in past analyses. Our measured ratio Fe XVIII $\lambda\lambda$16.078/15.265 gives a temperature of ~6 MK,

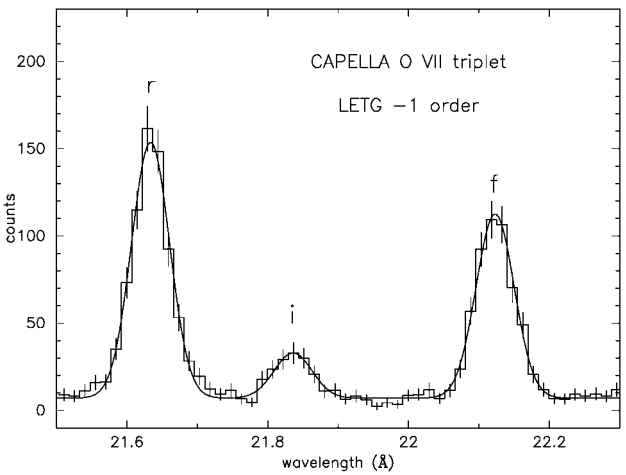

FIG. 2.—O VII triplet in the LETGS −1 order spectrum with the resonance (*r*), the forbidden (*f*), and the intercombination (*i*) line. The measured ratios of these lines (from the fitted curve) are given in the text.

and the photon flux ratio 15.014/15.265 is measured to be 2.64 ± 0.10. If we compare this to the recent EBIT results, we conclude that there is little or no evidence for opacity effects in the 15.014 Å line seen in our Capella spectrum.

4. CONCLUSION

The Capella measurements with LETGS show a rich spectrum with excellent spectral resolution ($\Delta\lambda \simeq 0.06$ Å, FWHM). About 150 lines have been identified, of which the brightest hundred are presented in Table 1. The high-resolution spectra of the *Chandra* grating spectrometers allow us to carry out direct density diagnostics using the He-like triplets of the most abundant elements in the LETGS band, which were previously only possible for the Sun. Density estimates based on C, N, and O He-like complexes indicate densities typical of solar active regions and some 2 or more orders of magnitude lower than density estimates for the hotter (>5 MK) plasma obtained from *EUVE* spectra. A preliminary investigation into the effect of resonance scattering in the Fe XVII line at 15.014 Å showed no clear evidence for opacity effects. After further LETGS in-flight calibration, it is expected that relative Doppler velocities of the order of 30 km s^{-1} will be detectable at the longest wavelengths.

The LETGS data as presented here could only be produced after dedicated efforts of many people for many years. Our special gratitude goes to the technical and scientific colleagues at SRON, MPE, and their subcontractors for making such a superb LETG and to the colleagues at many institutes for building the payload. Special thanks goes to the many teams who made *Chandra* a success, particularly the project scientist team, headed by Dr. Weisskopf, the MSFC project team, headed by Mr. Wojtalik, the TRW industrial teams and their subcontractors, the *Chandra* observatory team, headed by Dr. Tananbaum, and the crew of Space Shuttle flight STS-93.

J. J. D., O. J., M. J., V. K., S. S. M., D. P., P. R., and B. J. W. were supported by *Chandra* X-Ray Center NASA contract NAS8-39073 during the course of this research.

REFERENCES

Acton, L. W., Catura, R. C., Meyerott, A., & Wolfson, C. J. 1972, Sol. Phys., 26, 183
Bhatia, A. K., & Doschek, G. A. 1992, At. Data Nucl. Data Tables, 52, 1
Brickhouse, N. S., Raymond, J. C., & Smith, B. W. 1995, ApJS, 97, 551
Brinkman, A. C., et al. 1987, Astrophys. Lett. Commun., 26, 73
———. 1997, Proc. SPIE, 3113, 181
Brown, G. V., Beiersdorfer, P., Liedahl, D. A., & Widmann, K. 1998, ApJ, 502, 1015
Catura, R. C., Acton, L. W., & Johnson, H. M. 1975, ApJ, 196, L47
Dupree, A. K., Brickhouse, N. S., Doschek, G. A., Green, J. C., & Raymond, J. C. 1993, ApJ, 418, L41
Gabriel, A. H., & Jordan, C. 1969, MNRAS, 145, 241
Hummel, C. A., Armstrong, J. T., Quirrenbach, A., Buscher, D. F., Mozurkewich, D., Elias, N. M., II, & Wilson, R. E. 1994, AJ, 107, 1859
Mason, H. E., Bhatia, A. K, Kastner, S. O., Neupert, W. M., & Swartz, M. 1984, Sol. Phys., 92, 199
Mewe, R. 1991, A&A Rev., 3, 127
Mewe, R., Gronenschild, E. H. B. M., & van den Oord, G. H. J. 1985, A&AS, 62, 197
Mewe, R., Heise, J., Gronenschild, E. H. B. M., Brinkman, A. C., Schrijver, J., & den Boggende, A. J. F. 1975, ApJ, 202, L67
Mewe, R., Kaastra, J. S., & Liedahl, D. A. 1995, Legacy, 6, 16
Mewe, R., Lemen, J. R., & Schrijver, C. J. 1991, Ap&SS, 182, 35
Murray, S. S., et al. 1997, Proc. SPIE, 3114, 11
Phillips, K. J. H., Greer, C. J., Bhatia, A. K., Coffey, I. H., Barnsley, R., & Keenan, F. P. 1997, A&A, 324, 381
Phillips, K. J. H., Greer, C. J., Bhatia, A. K., & Keenan, F. P. 1996, ApJ, 469, L57
Phillips, K. J. H., Mewe, R., Harra-Murnion, L. K., Kaastra, J. S., Beiersdorf, P., Brown, G. V., & Liedahl, D. A. 1999, A&AS, 138, 381
Pradhan, A. K. 1982, ApJ, 263, 477
Predehl, P., et al. 1997, Proc. SPIE, 3113, 172
Saba, J. L. R., Schmelz, J. T., Bhatia, A. K., & Strong, K. T. 1999, ApJ, 510, 1064
Schrijver, C. J., Mewe, R., van den Oord, G. H. J., & Kaastra, J. S. 1995, A&A, 302, 438
Van Speybroeck, L. P., Jerius, D., Edgar, R. J., Gaetz, T. J., & Zhao, P. 1997, Proc. SPIE, 3113, 89
Wolfson, C. J., Doyle, J. G., & Phillips, K. J. H. 1983, ApJ, 269, 319